

AperTO - Archivio Istituzionale Open Access dell'Università di Torino

A model assessment of the role played by the carbonate (CO₃⁻) and dibromide (Br₂⁻) radicals in the photodegradation of glutathione in sunlit fresh- and salt-waters

This is the author's manuscript

Original Citation:

Availability:

This version is available <http://hdl.handle.net/2318/1687073> since 2019-01-17T12:47:50Z

Published version:

DOI:10.1016/j.chemosphere.2018.06.066

Terms of use:

Open Access

Anyone can freely access the full text of works made available as "Open Access". Works made available under a Creative Commons license can be used according to the terms and conditions of said license. Use of all other works requires consent of the right holder (author or publisher) if not exempted from copyright protection by the applicable law.

(Article begins on next page)

A model assessment of the role played by the carbonate ($\text{CO}_3^{\bullet-}$) and dibromide ($\text{Br}_2^{\bullet-}$) radicals in the photodegradation of glutathione in sunlit fresh- and salt-waters

Davide Vione^{1,2*}

¹ *Dipartimento di Chimica, Università di Torino, Via Pietro Giuria 5, 10125 Torino, Italy.*

² *Università di Torino, Centro Interdipartimentale NatRisk, Largo Paolo Braccini 2, 10095 Grugliasco (TO), Italy.*

* Corresponding author. E-mail: davide.vione@unito.it

Abstract

Glutathione (GLU) is a peptidic thiol that plays important anti-oxidant roles in organisms and that occurs in both freshwater and seawater, where it can undergo both bio- and photodegradation. Recent results have elucidated the role played by $\cdot\text{OH}$, $^1\text{O}_2$, H_2O_2 and other yet unidentified transients in GLU photochemistry, but very little is known of the role of $\text{CO}_3^{\bullet-}$. This is an important gap because $\text{CO}_3^{\bullet-}$ is usually very reactive towards electron-rich compounds including thiols and mercaptans. Very little is also known on the environmental importance of the reaction between GLU and $\text{Br}_2^{\bullet-}$, which could account for the literature finding that GLU phototransformation is enhanced in simulated seawater compared to freshwater. By means of a photochemical model approach based on the APEX software (Aqueous Photochemistry of Environmentally-occurring Xenobiotics), here we provide an assessment of the role that several photoreactants, including most notably $\text{CO}_3^{\bullet-}$ and $\text{Br}_2^{\bullet-}$, have in the photodegradation of GLU (both the whole substance and the

separate neutral and mono-anionic species) under representative fresh- and saltwater conditions. Our model suggests that $\text{CO}_3^{\bullet-}$ would dominate the photodegradation of GLU in low-DOC and high-pH freshwater. They are the only freshwater conditions that really ensure GLU photodegradation to be competitive with biotransformation. In surface seawater and in brackish water, GLU phototransformation would be dominated by the $\text{Br}_2^{\bullet-}$ reaction.

Keywords: peptidic thiols; environmental photochemistry; fresh-, brackish- and salt-water; sunlit surface waters; photoinduced transformation.

Introduction

Sulphur-containing peptides, or peptidic thiols, play an important role in biogeochemical cycles in natural waters. They are produced by micro-organisms for different purposes including detoxification, antioxidant action and redox processes (Paulsen and Carroll, 2013; Swarr et al., 2016). Once released in the extra-cellular environment, these compounds occur at sub-nM to nM concentration in the photic zone of natural waters and act as ligands for metals as well as precursors for CS_2 and COS (Grill et al., 1985; Dupont et al., 2006; Trogolo, 2016). Peptidic thiols are partially consumed by microbial processes (Wei and Ahner, 2005), but recent work suggests that they may also undergo important photochemical transformation.

Chu et al. (2017) have shown that important photodegradation is triggered by natural organic matter (NOM) via reactive intermediates such as $\bullet\text{OH}$, $^1\text{O}_2$ and H_2O_2 , and that a significant role is also played by still unidentified photochemical processes. While the cited work has contributed to shed new light on the environmental phototransformation of peptidic thiols, including the measurement

of several second-order reaction rate constants of key importance, there are still important issues that have not been answered. For instance, the used experimental conditions (no inorganic carbon occurring in the irradiated solutions) were not designed to study the reactivity of peptidic thiols with the carbonate radical, $\text{CO}_3^{\bullet-}$, which is another transient species of photochemical origin. Indeed, $\text{CO}_3^{\bullet-}$ is well known to play an important role in the degradation of electron-rich compounds such as some phenols, amines and, most notably, thiols and mercaptans (Neta et al., 1988; Huang and Mabury, 2000a/b).

The goal of this paper is to provide a model overview of the photochemical transformation of GLU in sunlit surface waters, with particular interest for the role of $\text{CO}_3^{\bullet-}$. Indeed, while this radical is known to take part to the environmental phototransformation of several sulphur-containing compounds, its role in the fate of GLU has been overlooked to our knowledge. To compare our model predictions with experimental data we took as reference the results of Chu et al. (2017), who have thoroughly characterised many photochemical transformation pathways of GLU with the notable exception of $\text{CO}_3^{\bullet-}$.

Photochemical reactions play a key role in the degradation of both xenobiotics and naturally occurring compounds in sunlit environmental waters. The direct photolysis, which is hardly operational with natural peptidic thiols, involves the absorption of sunlight by the substrate that undergoes photodegradation as a consequence (Richard and Hoffmann, 2016). In contrast, indirect photochemistry is triggered by the absorption of sunlight by natural molecules called photosensitisers, of which the most important are the chromophoric dissolved organic matter (CDOM, which largely overlaps with the chromophoric fraction of NOM), nitrate and nitrite (McKay and Rosario-Ortiz, 2016). Sunlight-irradiated CDOM produces reactive triplet states ($^3\text{CDOM}^*$) that then react with dissolved oxygen to produce $^1\text{O}_2$, while $\bullet\text{OH}$ is produced by still insufficiently characterised processes involving irradiated CDOM (one of which involves

photogenerated H_2O_2 ; McNeill and Canonica, 2016; Rosario-Ortiz and Canonica, 2016), as well as by nitrate and nitrite under irradiation (Vione et al., 2014; Gligorovski et al., 2015). Moreover, the oxidation of carbonate and bicarbonate by $\bullet\text{OH}$ and (usually to a minor extent) the oxidation of CO_3^{2-} by $^3\text{CDOM}^*$ are photochemical sources of $\text{CO}_3^{\bullet-}$ (Canonica et al., 2005). Since some years it is possible to model these processes thanks to the development of a software (APEX: Aqueous Photochemistry of Environmentally-occurring Xenobiotics; Bodrato and Vione, 2014), by which we have been able to reproduce the photochemical lifetimes of several compounds such as pharmaceuticals, pesticides and personal care products. As input data, APEX requires photochemical reactivity parameters of the substrate undergoing photodegradation (second-order rate constants between substrates and reactive transient species) and environmental features such as sunlight irradiance, water chemistry and depth. In the present work we chose the sulphur-containing tripeptide glutathione (GLU) as study compound, because a relatively complete dataset of its photoreactivity parameters is available in the literature. Data availability (Encinas et al., 1985; Buxton et al., 1988; Neta et al., 1988; Chu et al., 2017) allows for the photochemical modelling of the environmental photo-fate of this compound. GLU can occur in two forms in natural waters, namely the acidic (GSH, $\text{pK}_a = 9.3$) and the basic one (GS^-) (Ibarra et al., 2001), and most of the needed photochemical parameters are available for both forms.

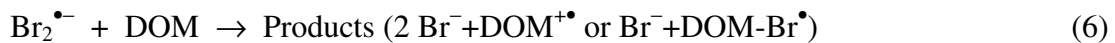
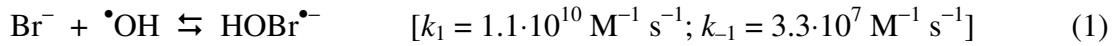
Methods

The phototransformation kinetics of GLU was modelled with the APEX software, considering fair-weather, mid-latitude sunlight irradiation and conditions (water chemistry, depth) that are reasonable for surface-water environments. In addition to predicting the overall phototransformation kinetics, APEX is also able to assess the importance of the different photochemical pathways as a function of variable environmental conditions. An issue to be highlighted concerns the modelled reactions with $\text{CO}_3^{\bullet-}$. The formation of $\text{CO}_3^{\bullet-}$ takes place mainly because of the reaction between $\bullet\text{OH}$ and $\text{HCO}_3^-/\text{CO}_3^{2-}$ and, usually to a lesser extent, upon oxidation of CO_3^{2-} by ${}^3\text{CDOM}^*$ (Buxton et al., 1988; Vione et al., 2014). Estimates of the second-order reaction rate constant of the latter process are available in the literature, but they vary widely (Canonica et al., 2005). Therefore, to avoid possible over-predictions of the importance of the $\text{CO}_3^{\bullet-}$ process, we decided not to consider the reaction between CO_3^{2-} and ${}^3\text{CDOM}^*$. By so doing, we obtain a lower limit for the steady-state $[\text{CO}_3^{\bullet-}]$.

To obtain a closer match with the environmental conditions we assumed typical concentration values of nitrate, nitrite and inorganic carbon. However, we did not include these components in the model simulations that were intended to match the experimental results of Chu et al. (2017), who irradiated GLU in the presence of humic substances with $\text{DOC} = 11.4 \text{ mg}_C \text{ L}^{-1}$. A relevant issue to be considered when comparing model predictions with experimental data is that GLU also undergoes an important reaction with H_2O_2 . Unfortunately, to date it is not yet possible to predict the occurrence of H_2O_2 in natural waters because, while the formation rates and quantum yields are reasonably well known even on a global scale (Powers and Miller, 2014; Kieber et al., 2014), knowledge of the decay kinetics for the assessment of the steady-state $[\text{H}_2\text{O}_2]$ is lagging much behind. Considering that H_2O_2 is mainly involved in the photodegradation of GS^- and it is thus

mostly operational at basic pH (Chu et al., 2017), the inability to take the H₂O₂ pathway into account leads to an underestimation of the GS⁻ reactivity and, as a consequence, of the GLU phototransformation kinetics under basic conditions.

We also considered the reaction between GLU and Br₂^{•-}, which could be important in brackish or seawater where a significant occurrence of the dibromide radical is expected (Parker and Mitch, 2016). The steady-state [Br₂^{•-}] was calculated here on the basis of Br[•]/Br₂^{•-} formation upon Br⁻ oxidation by [•]OH and ³CDOM*, and of Br₂^{•-} transformation by disproportionation and reactions with nitrite and DOM (DOM represents the whole pool of the dissolved organic matter, either chromophoric or not; Zehavi and Rabani, 1972; Buxton et al., 1988; Neta et al., 1988; Von Gunten and Hoigné, 1996; De Laurentiis et al., 2012).



The oxidation reaction (3) of bromide by ³CDOM* is potentially important (De Laurentiis et al., 2012; Parker and Mitch, 2016), but its rate constant is still poorly known. A rough estimate by using CDOM proxies is available as $k_3 = 3.5 \cdot 10^9 \text{ M}^{-1} \text{ s}^{-1}$ (De Laurentiis et al., 2012), but there is evidence that such a value is an overestimate of the actual rate constant (Parker and Mitch, 2016). In the present work, we used the experimental data of Chu et al. (2017) to obtain an estimate of k_3 that could then be used in the following model simulations.

The rate constant of reaction (6) is also not exactly known, but an estimate may be obtained by considering the reaction rate constants between $\text{Br}_2^{\bullet-}$ and phenolic compounds ($k_6 = 2 \cdot 10^7 \text{ M}^{-1} \text{ s}^{-1}$ or, in more manageable units, $k_6 = 3 \cdot 10^2 \text{ L (mg}_C\text{)}^{-1} \text{ s}^{-1}$; De Laurentiis et al., 2012). The $\text{mg}_C \text{ L}^{-1}$ units are more straightforward to use than the molar ones when the DOM is measured as the dissolved organic carbon (DOC, expressed in $\text{mg}_C \text{ L}^{-1}$). Our estimate of k_6 is probably an upper limit, because phenolic compounds are more reactive than average organic molecules toward $\text{Br}_2^{\bullet-}$ (Neta et al., 1988). Therefore, by overestimating the $\text{Br}_2^{\bullet-}$ consumption by DOM we obtain a lower limit for the steady-state $[\text{Br}_2^{\bullet-}]$ under environmental conditions. From the reaction sequence (1-7), by applying the steady-state approximation to $\text{HOBr}^{\bullet-}$, Br^{\bullet} and $\text{Br}_2^{\bullet-}$ one gets the following system of equations:

$$\begin{cases} \frac{d[\text{HOBr}^{\bullet-}]}{dt} = 0 = k_1[\bullet\text{OH}][\text{Br}^-] - (k_{-1} + k_2)[\text{HOBr}^{\bullet-}] \\ \frac{d[\text{Br}^{\bullet}]}{dt} = 0 = k_2[\text{HOBr}^{\bullet-}] - k_4[\text{Br}^-][\text{Br}^{\bullet}] \\ \frac{d[\text{Br}_2^{\bullet-}]}{dt} = 0 = k_4[\text{Br}^-][\text{Br}^{\bullet}] - 2k_5[\text{Br}_2^{\bullet-}]^2 - k_6 \text{DOC}[\text{Br}_2^{\bullet-}] - k_7[\text{NO}_2^-][\text{Br}_2^{\bullet-}] \end{cases} \quad (8)$$

Note that, by summing together the second and third equations, the term $k_4[\text{Br}^-][\text{Br}^{\bullet}]$ gets cancelled and the knowledge of k_4 is, therefore, not necessary. The system of equations has the following solution, where the quadratic term is introduced by reaction (5):

$$[\text{Br}_2^{\bullet-}] = \frac{-(k_6 \text{DOC} + k_7[\text{NO}_2^-]) + \sqrt{(k_6 \text{DOC} + k_7[\text{NO}_2^-])^2 + 8k_5[\text{Br}^-](k_1k_2(k_{-1} + k_2)^{-1}[\bullet\text{OH}] + k_3[{}^3\text{CDOM}^*])}}{4k_5} \quad (9)$$

The assessment of $[\bullet\text{OH}]$ and $[{}^3\text{CDOM}^*]$ as input data in equation (9) was carried out with the APEX software. The software takes into account the generation of $\bullet\text{OH}$ by irradiated CDOM, nitrate and nitrite, as well as $\bullet\text{OH}$ scavenging by DOM, bicarbonate, carbonate, nitrite and bromide (Bodrato and Vione, 2014). As far as ${}^3\text{CDOM}^*$ is concerned, APEX considers its photogeneration by irradiated CDOM and the typical ${}^3\text{CDOM}^*$ decay kinetics that are observed in aerated natural

waters (McNeill and Canonica, 2016). In the present case, the APEX predictions were corrected for the reaction between ${}^3\text{CDOM}^*$ and Br^- . To predict the photodegradation kinetics of GLU, in addition to the steady-state concentrations of the photogenerated transients, one should also consider the reactivity of the GLU species GSH and GS^- . **Table 1** reports the available literature values for the reaction rate constants between GLU (i.e., GSH and GS^- separately) and several transient species ($\bullet\text{OH}$, ${}^1\text{O}_2$, $\text{CO}_3^{\bullet-}$, triplet states, $\text{Br}_2^{\bullet-}$) that may be responsible for photoinduced degradation in freshwater and seawater. GLU is known to react with $\bullet\text{OH}$, ${}^1\text{O}_2$ and $\text{CO}_3^{\bullet-}$, for which processes the second-order reaction rate constants are known from the literature for both GSH and GS^- (Neta et al., 1988; Mezyk et al., 1996; Chu et al., 2017). As far as triplet sensitisation is concerned, the reaction rate constants with the triplet states of model triplet sensitisers are usually available instead of the ${}^3\text{CDOM}^*$ rate constants, which are much more difficult and uncertain to determine. The case of GLU makes no exception and the literature reports the quenching rate constants with the triplet state of benzophenone (${}^3\text{BP}^*$), which has been shown previously to be a good ${}^3\text{CDOM}^*$ proxy (Avetta et al., 2016). The quenching rate constants are very similar for both GSH and GS^- (Encinas et al., 1985; $k_{\text{GLU},{}^3\text{BP}^*} = 6.7 \times 10^8 \text{ L mol}^{-1} \text{ s}^{-1}$). However, the one-electron oxidation of an organic substrate by ${}^3\text{BP}^*$ yields an ion couple between the reduced BP and the oxidised substrate (Hurley et al., 1988), which can either evolve into reaction products or give back BP and the original substrate (GSH or GS^- in the present case). The second phenomenon does not lead to transformation, and for this reason the quenching rate constants are actually upper limits for the reaction rate constants (Bortolus et al., 1989). Note that the decay of ${}^3\text{CDOM}^*$ in freshwaters mainly takes place upon reaction with O_2 and through internal conversion, while the reaction with organic substrates such as GLU usually plays a minor role (McNeill and Canonica, 2016). This means that the value of $k_{\text{GLU},{}^3\text{CDOM}^*}$ affects the GLU phototransformation kinetics but not the steady-state [${}^3\text{CDOM}^*$].

In the case of $\text{Br}_2^{\bullet-}$, only the reaction rate constant with GSH is available (Neta et al., 1988). Therefore, the model assessment of the effect of bromide on GLU photodegradation was carried out for GSH alone. A final issue is that the standard time unit used in APEX is a summer sunny day, the average irradiance of which is equivalent to fair-weather 15 July at mid latitude. This time unit is used in all the model predictions of GLU phototransformation under environmental conditions.

Results and Discussion

Model validation against literature experimental data

As mentioned above, we used the experimental results of Chu et al. (2017) as reference for our photochemical model, to test and validate the model assumptions before extending them to more general environmental conditions. A difficulty is represented by the fact that the cited authors used UVA radiation as well as peculiar irradiation set-up and optical path lengths, which are either not specified or not easily reproduced by the model. However, by normalising the experimental data it is possible to focus on the trend of the GLU photodegradation kinetics rather than on the absolute values of its transformation rate constants. In this way, it is still possible to get a validation of key model parameters while bypassing most of the problems mentioned above. Our photochemical model does not take the H_2O_2 reaction into account, but Chu et al. (2017) have provided a detailed account of the role of the different processes in GLU phototransformation at different pH values. Therefore, it is possible to test our model against the H_2O_2 -independent photoreaction pathways.

A comparison between our model predictions and the experimental data reported by Chu et al. (2017) for the GLU phototransformation kinetics as a function of pH, accounted for by $\bullet\text{OH}$ and $^1\text{O}_2$

is provided in **Figure 1a**. The GLU rate constants reported in the figure are all normalised to the experimental rate constant value at pH 7 (hereafter, k_7). To enable the comparison between model and experiments, in the model we assumed the occurrence of organic matter alone without nitrate, nitrite or inorganic carbon as additional species of photochemical significance. A close agreement between model and experiments could be obtained by assuming $[^1\text{O}_2] [\bullet\text{OH}]^{-1} = 190$, and the figure also shows that the experimental data at $\text{pH} > 8$ are not consistent with steady-state concentration ratios equal to, say, 100 or 300. This issue provides insight into the robustness of the comparison of model predictions with experimental data. To obtain $[^1\text{O}_2] [\bullet\text{OH}]^{-1} = 190$ in the model simulations, in the presence of $\text{DOC} = 11.4 \text{ mg}_C \text{ L}^{-1}$ as per the experimental conditions of Chu et al. (2017), one has to assume $\Phi_{^1\text{O}_2} (\Phi_{\bullet\text{OH}})^{-1} = 83$.

Chu et al. (2017) have not singled out the $^3\text{CDOM}^*$ contribution to GLU photodegradation in their experimental results but, given the significant reactivity between GLU and $^3\text{BP}^*$ and the use of model humic substances in the relevant irradiation experiments, we strongly suspect that the “other processes” quantified by the cited authors are mainly accounted for by $^3\text{CDOM}^*$. By comparing experimental data with model predictions one can thus obtain an estimate of the second-order reaction rate constant between GLU and $^3\text{CDOM}^*$, provided that a hypothesis is made on the ratio of $[^1\text{O}_2] [^3\text{CDOM}^*]^{-1}$ (or of $\Phi_{^1\text{O}_2} (\Phi_{^3\text{CDOM}^*})^{-1}$). In irradiated solutions of humic substances one often finds that $[^1\text{O}_2] \sim [^3\text{CDOM}^*]$ (McNeill and Canonica, 2016). The decay kinetics of $^3\text{CDOM}^*$ in aerated solution is largely accounted for by O_2 quenching that produces $^1\text{O}_2$ with a yield that is estimated at around 50% (Mcneill and Canonica, 2016) and leads to a first-order decay constant for $^3\text{CDOM}^*$ of around $5 \times 10^5 \text{ s}^{-1}$ (Cannonica and Freiburghaus, 2001), which is double as compared to the rate constant of $^1\text{O}_2$ quenching by collision with water ($2.5 \times 10^5 \text{ s}^{-1}$) (Wilkinson et al., 1995). We thus assumed $[^1\text{O}_2] = [^3\text{CDOM}^*]$ and $\Phi_{^3\text{CDOM}^*} = 2 \Phi_{^1\text{O}_2}$, and considered the experimental first-order rate constant of GLU phototransformation accounted for by unknown processes (Chu et al.,

2017), which in the pH range of 7 to 10 can be compared well with our model predictions. A normalisation procedure was here required as well and, to obtain an overall consistency in data treatment, we normalised the new data using the same k_7 value as above that is referred to the sum of the (experimental or modelled) GLU degradation rate constants by $^1\text{O}_2$ and $\bullet\text{OH}$ at pH 7. After the normalisation procedure, the comparison between experimental data and model predictions (see **Figure 1b**) yielded the second-order reaction rate constant $k_{GLU,^3CDOM^*} = 8 \times 10^7 \text{ L mol}^{-1} \text{ s}^{-1}$. A modification of the rate constant by $\pm 25\%$ would produce a poor consistency between model and experiments, and there is little indication from the experimental data that the rate constant $k_{GS^-,^3CDOM^*}$ may be considerably different from $k_{GSH,^3CDOM^*}$. We thus assumed that the two rate constants are equal, which is consistent with the literature data of the quenching constant $k_{GLU,^3BP^*}$ that is very similar between GSH and GS^- (Encinas et al., 1985). However, the quenching constant $k_{GLU,^3BP^*}$ is almost an order of magnitude higher than the reaction rate constant $k_{GLU,^3CDOM^*}$. In addition to the correctness of our identification of unknown processes with $^3CDOM^*$, and to how much $^3BP^*$ is representative of $^3CDOM^*$, such a difference is reasonable when comparing quenching and reaction rate constants because the quenching phenomena do not necessarily lead to net transformation, and one order-of-magnitude differences are actually reported in the literature (Minella et al., in press).

From some of the above assumptions and the comparison between model and experiments we have $\Phi_{^3CDOM^*} = 2 \Phi_{^1O_2} = 165 \Phi_{\bullet OH}$, which were then used as APEX input data to assess the phototransformation kinetics and pathways of GLU in a variety of environmentally significant conditions. The need to use a normalisation procedure prevents absolute quantum yield values to be obtained from the experimental data of Chu et al. (2017), but other works suggest that under UVA irradiation one has $\Phi_{^1O_2} \sim 0.01$ (Marchisio et al., 2015). In this way it is possible to derive the

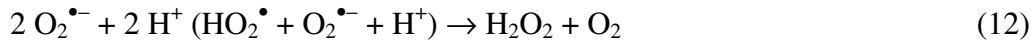
corresponding values for $\Phi_{^3\text{CDOM}^*}$ and $\Phi_{\bullet\text{OH}}$, and to obtain a complete set of input data for APEX modelling.

Modelling GLU phototransformation kinetics and pathways in freshwater

After validation of the model parameters, it is possible to use APEX to assess the photochemical fate of GLU under environmentally relevant conditions. A first set of predictions is reported in **Figure 2**, and it is referred to the two species GSH and GS^- taken separately. Each figure panel reports the overall photodegradation kinetics (accounted for by $\bullet\text{OH}$, $\text{CO}_3^{\bullet-}$, $^1\text{O}_2$ and $^3\text{CDOM}^*$, thereby excluding the contribution of H_2O_2), as well as the contribution of the single photoreaction pathways. The case of GSH as a function of the DOC is reported in **Figure 2a**. It is evident that GSH phototransformation is 2-3 times faster at low DOC (lifetime of a couple of weeks or shorter) than at high DOC (one-month lifetime or longer). The prevailing photoreactions are those with $\bullet\text{OH}$ at low DOC and with $^3\text{CDOM}^*$ at high DOC. The corresponding plot for GS^- (**Figure 2b**) suggests that $\text{CO}_3^{\bullet-}$ plays an important role at low DOC. At high DOC one expects important photodegradation by $^1\text{O}_2$, with significant contributions of $\text{CO}_3^{\bullet-}$ (decreasing with increasing DOC) and $^3\text{CDOM}^*$ (increasing with DOC). Note that for both GSH and GS^- the importance of $\bullet\text{OH}$ and $\text{CO}_3^{\bullet-}$ decreases with increasing DOC, while the opposite happens with $^1\text{O}_2$ and $^3\text{CDOM}^*$. The reason is that $\bullet\text{OH}$ and $\text{CO}_3^{\bullet-}$ are largely scavenged by DOM that keeps their steady-state concentrations low at high DOC, while CDOM under irradiation produces both $^3\text{CDOM}^*$ and $^1\text{O}_2$ (Vione et al., 2014).

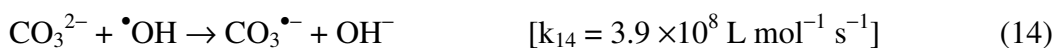
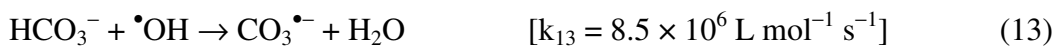
GS^- would also react with H_2O_2 to a considerable extent (Chu et al., 2017) and, considering that H_2O_2 is a by-product of $^3\text{CDOM}^*$ photoreactions (see reactions (10-12), where S is a generic substrate; Sur et al., 2011), its importance should be enhanced at high DOC. Chu et al. (2017),

operating at $\text{DOC} = 11.4 \text{ mg}_C \text{ L}^{-1}$ report that the reaction with H_2O_2 is comparable to that with $^1\text{O}_2$ at basic pH. Therefore, it is very likely that GS^- photodegradation is dominated by $\text{CO}_3^{\bullet-}$ at low DOC and by $\text{H}_2\text{O}_2/^1\text{O}_2$ at high DOC.



A comparison between **Figure 2a** (GSH) and **Figure 2b** (GS^-) suggests that GS^- has shorter lifetime than GSH. GSH and GS^- have the same (or very similar) reaction rate constants with $^3\text{CDOM}^*$, and the resulting first-order degradation rate constants are equal as well. However, while $^3\text{CDOM}^*$ plays a major role in GSH phototransformation, its relative role is much lower in the case of GS^- because of the faster overall transformation kinetics. The photolability of GS^- is evident even by neglecting the H_2O_2 process; if the reaction between GS^- and H_2O_2 were considered, the lifetime difference between GS^- and GSH would be even higher.

A major goal of this work is the assessment of the role of $\text{CO}_3^{\bullet-}$, the formation of which requires the occurrence of inorganic carbon (carbonate and bicarbonate) for the oxidation reactions by $^{\bullet}\text{OH}$ to be operational (Buxton et al., 1988; Canonica et al., 2005; Vione et al, 2014):



Therefore, it is interesting to see the impact of inorganic carbon concentration ($[\text{HCO}_3^-] + [\text{CO}_3^{2-}]$) on the pathways and kinetics of GSH/ GS^- phototransformation. To run the model we assumed $\text{DOC} = 5 \text{ mg}_C \text{ L}^{-1}$ and $[\text{HCO}_3^-] = 100 [\text{CO}_3^{2-}]$ (pH ~ 8.3). GSH is poorly affected by the $\text{CO}_3^{\bullet-}$ process (see **Figure 2c**), and its phototransformation kinetics practically does not vary with varying

$[\text{HCO}_3^-] + [\text{CO}_3^{2-}]$. In contrast, the photodegradation of GS^- gets faster as the inorganic carbon increases and as the role of $\text{CO}_3^{\bullet-}$ becomes more important (**Figure 2d**).

The importance of $\text{CO}_3^{\bullet-}$ as photoreaction pathway compared to $\bullet\text{OH}$ depends on the competition kinetics between the substrate (GSH or GS^-) and DOM for reaction with $\bullet\text{OH}/\text{CO}_3^{\bullet-}$. The reaction rate constant between $\text{CO}_3^{\bullet-}$ and DOM is over two orders of magnitude lower than the corresponding $\bullet\text{OH}$ rate constant (Vione et al., 2014), but DOM inhibits the occurrence of $\text{CO}_3^{\bullet-}$ twice: first by scavenging $\bullet\text{OH}$ that is required for $\text{CO}_3^{\bullet-}$ formation, and then by directly consuming $\text{CO}_3^{\bullet-}$. Therefore, one usually has $[\bullet\text{OH}] \propto \text{DOC}^{-1}$ and $[\text{CO}_3^{\bullet-}] \propto \text{DOC}^{-2}$. At low DOC the slower reaction with DOM favours $\text{CO}_3^{\bullet-}$ over $\bullet\text{OH}$, but at high DOC the scenario can change. **Figure 3** reports the ratio $[\text{CO}_3^{\bullet-}] / [\bullet\text{OH}]^{-1}$ as a function of $[\text{HCO}_3^-] + [\text{CO}_3^{2-}]$ for different DOC values (up to $10 \text{ mg}_C \text{ L}^{-1}$). The ratio increases with increasing $[\text{HCO}_3^-] + [\text{CO}_3^{2-}]$ and with decreasing DOC, as expected, and for all considered DOC values it is $[\text{CO}_3^{\bullet-}] > [\bullet\text{OH}]$ if $[\text{HCO}_3^-] + [\text{CO}_3^{2-}] > 0.1 \text{ mmol L}^{-1}$. Because of the much lower reaction rate constant with DOM of $\text{CO}_3^{\bullet-}$ compared to $\bullet\text{OH}$, $[\text{CO}_3^{\bullet-}]$ can even be a couple of orders of magnitude higher than $[\bullet\text{OH}]$ provided that $[\text{HCO}_3^-] + [\text{CO}_3^{2-}]$ is high enough and the DOC is low. However, under opposite conditions one can have $[\bullet\text{OH}] > [\text{CO}_3^{\bullet-}]$.

In the case of GSH it is $k_{\text{GSH},\bullet\text{OH}} (k_{\text{GSH},\text{CO}_3^{\bullet-}})^{-1} \sim 600$, thus for $\text{CO}_3^{\bullet-}$ to prevail over $\bullet\text{OH}$ in GSH photodegradation one needs $[\text{CO}_3^{\bullet-}] > 600 [\bullet\text{OH}]$, which would hardly ever occur (see **Figure 3**). In contrast, for GS^- it is $k_{\text{GS}^-,\bullet\text{OH}} (k_{\text{GS}^-,\text{CO}_3^{\bullet-}})^{-1} \sim 1.3$ and it is quite easy to have $[\text{CO}_3^{\bullet-}] > 1.3 [\bullet\text{OH}]$. In the scenario reported in **Figure 2d**, with $\text{DOC} = 5 \text{ mg}_C \text{ L}^{-1}$ and $[\text{HCO}_3^-] + [\text{CO}_3^{2-}] = 1 \text{ mmol L}^{-1}$, the ions HCO_3^- and CO_3^{2-} induce a replacement of $\bullet\text{OH}$ with $\text{CO}_3^{\bullet-}$ as reactive radical species, and the overall importance of the combined ($\bullet\text{OH} + \text{CO}_3^{\bullet-}$) process in GS^- degradation increases as the

$\text{CO}_3^{\bullet-}$ pathway is enhanced. The reason is that $\text{CO}_3^{\bullet-}$ undergoes lesser scavenging than $\bullet\text{OH}$ by DOM, which induces a more efficient GS^- degradation.

It is also interesting to assess the role of the carbonate radical in the acceleration of GLU photodegradation with increasing pH. We carried out model calculations for $[\text{HCO}_3^-] + [\text{CO}_3^{2-}] = 1$ mmol L^{-1} and for two different values of the DOC, namely 1 $\text{mg}_\text{C} \text{L}^{-1}$ (hereafter low-DOC conditions, **Figure 4a**) and 10 $\text{mg}_\text{C} \text{L}^{-1}$ (hereafter high-DOC conditions, **Figure 4b**). Under low-DOC conditions, our model results clearly suggest that the photodegradation kinetics of GLU gets faster as the pH increases because of the growing importance of the $\text{CO}_3^{\bullet-}$ pathway. There are mainly two reasons for this result: (i) with increasing pH one has an increase in $[\text{CO}_3^{2-}]$ at the expense of $[\text{HCO}_3^-]$, and the reaction between $\bullet\text{OH}$ and CO_3^{2-} to give $\text{CO}_3^{\bullet-}$ is faster than the process involving HCO_3^- . With increasing pH one has a decrease of $[\bullet\text{OH}]$ (which is reflected in the decreasing importance of the $\bullet\text{OH}$ transformation pathway, see **Figure 4a**) and an increase of $[\text{CO}_3^{\bullet-}]$, which causes faster GLU phototransformation because the $\text{CO}_3^{\bullet-}$ process is more efficient at low DOC as explained above; (ii) with increasing pH one has also a higher occurrence of GS^- at the expense of GSH, and GS^- is considerably more reactive than GSH towards $\text{CO}_3^{\bullet-}$. The outcome is that $\text{CO}_3^{\bullet-}$ dominates the photodegradation of GLU above pH 8 under low-DOC conditions, where it is also unlikely that H_2O_2 plays a key role in the degradation process.

In the case of high-DOC conditions (**Figure 4b**), which are little favourable to the occurrence of $\text{CO}_3^{\bullet-}$, one has a replacement of the $\bullet\text{OH}$ pathway with $\text{CO}_3^{\bullet-}$ as the pH increases but the overall kinetics of the combined ($\bullet\text{OH} + \text{CO}_3^{\bullet-}$) process is not much modified, and its role is just a secondary one. In contrast the $^3\text{CDOM}^*$ pathway is always important, and the increase in the GLU degradation rate constant with increasing pH is accounted for by the $^1\text{O}_2$ process (GS^- reacts with $^1\text{O}_2$ almost one hundred times faster than GSH). It is reasonable to find an important role of

$^3\text{CDOM}^*$ and $^1\text{O}_2$ at high DOC because, as mentioned before, both $[^3\text{CDOM}^*]$ and $[^1\text{O}_2]$ increase with increasing DOC. On the basis of the experimental data of Chu et al. (2017) one can additionally infer that, in the real world, the pH increase of the GLU photodegradation rate constant would be even higher because of the additional role of the H_2O_2 reaction with GS^- .

In the case of freshwaters, $\text{CO}_3^{\bullet-}$ would play a major role in GLU degradation at $\text{pH} > 8$ in low-DOC conditions. Below $\text{pH} 8$ the photodegradation would be dominated by $\bullet\text{OH}$ but with slow overall kinetics. Because the biodegradation lifetime of GLU is expected to be in the range of 3-5 days (Leggatt et al., 2007), biodegradation has several chances to prevail over photodegradation at $\text{pH} < 8$. At high DOC one expects an important role of $^3\text{CDOM}^*$ in the photodegradation of GLU, but the $^3\text{CDOM}^*$ process alone gives a GLU lifetime of about one month that would not be competitive with biodegradation. The modelled GLU photodegradation kinetics becomes faster above $\text{pH} 8$ because of the $^1\text{O}_2$ process, but one needs an environmentally unlikely $\text{pH} > 9$ for the $^1\text{O}_2$ reaction to overcome the $^3\text{CDOM}^*$ one. However, at high DOC one expects faster GLU photodegradation because of the H_2O_2 reaction as well (Chu et al., 2017). Interestingly, the fastest GLU photodegradation (with 2 - 10 days lifetime) is found for $\text{pH} > 8$ and low DOC, where $\text{CO}_3^{\bullet-}$ is by far the main reactive species. The radical $\text{CO}_3^{\bullet-}$ is thus predicted to dominate GLU phototransformation in freshwaters, exactly under the conditions where photochemistry is expected to be most important. Note that elevated pH values can be reached during summertime in the presence of a strong photosynthetic activity that consumes CO_2 (Mostofa et al., 2016).

Modelling GLU photodegradation in saltwater

Our modelling of GLU photodegradation in saltwater took the $\text{Br}_2^{\bullet-}$ reaction into account. As already mentioned, only the reaction rate constant between GSH and $\text{Br}_2^{\bullet-}$ is available (see **Table 1**)

and we carried out model calculations in the case of GSH alone. First of all we validated the model against the experimental data of Chu et al. (2017), who studied GLU photodegradation under ~neutral conditions with varying salinity. The most uncertain parameter in photochemical modelling is the reaction rate constant between Br^- and ${}^3\text{CDOM}^*$ ($k_{\text{Br}^-, {}^3\text{CDOM}^*}$), and we used the normalised experimental data (normalised with respect to the GSH photodegradation rate constant in the absence of added salts) to get an estimate of $k_{\text{Br}^-, {}^3\text{CDOM}^*}$. The first-order photodegradation rate constant of GSH was assessed in the model based on the reactions with $\bullet\text{OH}$, $\text{CO}_3^{\bullet-}$, ${}^1\text{O}_2$, ${}^3\text{CDOM}^*$ and $\text{Br}_2^{\bullet-}$, using the second-order reaction rate constants between GSH and each relevant transient species, as well as the transient steady-state concentrations:

$$k_{\text{GSH}} = k_{\text{GSH}, \bullet\text{OH}} [\bullet\text{OH}] + k_{\text{GSH}, \text{CO}_3^{\bullet-}} [\text{CO}_3^{\bullet-}] + k_{\text{GSH}, {}^1\text{O}_2} [{}^1\text{O}_2] + k_{\text{GSH}, {}^3\text{CDOM}^*} [{}^3\text{CDOM}^*] + k_{\text{GSH}, \text{Br}_2^{\bullet-}} [\text{Br}_2^{\bullet-}] \quad (15)$$

where $[\text{Br}_2^{\bullet-}]$ is expressed by equation (9). In agreement with experimental conditions we assumed $\text{DOC} = 11.4 \text{ mg}_\text{C} \text{ L}^{-1}$ and no nitrate, nitrite or inorganic carbon. We derived $[\bullet\text{OH}]$, $[\text{CO}_3^{\bullet-}]$, $[{}^1\text{O}_2]$ and $[{}^3\text{CDOM}^*]$ as APEX output parameters, but corrected $[{}^3\text{CDOM}^*]$ for the additional reaction with Br^- that adds to the other ${}^3\text{CDOM}^*$ decay pathways (an iterative calculation applies here). The comparison between model predictions and the experimental data of Chu et al. (2017) is reported in **Figure 5a**, and a good agreement could be reached with $k_{\text{Br}^-, {}^3\text{CDOM}^*} = (1.2 \pm 0.6) \times 10^7 \text{ L mol}^{-1} \text{ s}^{-1}$. The figure shows that the agreement with the experimental data is lost if one increases or decreases $k_{\text{Br}^-, {}^3\text{CDOM}^*}$ by a ~2 factor. To match the experimental data we assumed that $\text{Br}_2^{\bullet-}$ is the only additional reactive species that occurs in saltwater as compared with freshwater. No formation of $\text{Cl}^\bullet/\text{Cl}_2^{\bullet-}$ is expected to occur at the seawater pH values upon reaction between $\bullet\text{OH}$ and Cl^- (Buxton et al., 1988), but there is evidence that ${}^3\text{CDOM}^*$ can oxidise Cl^- (Parker and Mitch, 2016). Little is known about the relevant reaction rate constant, except for an upper-limit estimate obtained by using anthraquinone-2-sulphonate as CDOM proxy (Brigante et al., 2014). For this reason we

did not include the formation and reactivity of $\text{Cl}_2^{\bullet-}$ in the model and, if some GSH degradation is actually induced by $\text{Cl}_2^{\bullet-}$, our value of $k_{\text{Br}^-, \text{CDOM}^*}$ overestimates the actual reaction rate constant. Our $k_{\text{Br}^-, \text{CDOM}^*}$ value could in fact include the $\text{Cl}_2^{\bullet-}$ -induced degradation as well.

For environmental modelling we assumed $0.1 \text{ mmol L}^{-1} \text{ NO}_3^-$, $1 \text{ } \mu\text{mol L}^{-1} \text{ NO}_2^-$, $1 \text{ mg}_C \text{ L}^{-1} \text{ DOC}$ (in agreement with the oligotrophic conditions that are usually found in seawater; Mostofa et al., 2016), $1 \text{ mmol L}^{-1} \text{ HCO}_3^-$ and $10 \text{ } \mu\text{mol L}^{-1} \text{ CO}_3^{2-}$ (thereby assuming $\text{pH} \sim 8.3$, in reasonable agreement with seawater conditions). **Figure 5b** reports the results of the modelling simulation of GSH first-order photodegradation rate constant as a function of salinity. Note that the typical seawater conditions highlighted on the plot correspond to 3.5% salinity and $0.8 \text{ mmol L}^{-1} \text{ Br}^-$ (Mostofa et al., 2016). The $\bullet\text{OH}$ process is inhibited with increasing salinity because of the scavenging of $\bullet\text{OH}$ by Br^- , while the $\text{Br}_2^{\bullet-}$ reaction is understandably enhanced. Relatively low $[\text{Br}^-]$ (corresponding to 0.2% salinity or less) would be already sufficient to make the $\text{Br}_2^{\bullet-}$ reaction prevail over the other GSH phototransformation pathways. The balance between $\bullet\text{OH}$ inhibition and $\text{Br}_2^{\bullet-}$ enhancement produced a slight increase of GSH degradation with salinity, which is different from the experimental data of Chu et al. (2017) (see **Figure 5a**) because the cited authors operated at high DOC without nitrate or nitrite. These experimental conditions are highly unfavourable to the $\bullet\text{OH}$ reaction, even at low salinity. Therefore, in the real world salinity can enhance the photodegradation of GSH, but particular conditions (high DOC, low nitrate and nitrite) are required for the salinity effect to be as important as suggested by the experimental data of Chu et al. (2017).

Also note that we did not consider the $\text{Cl}_2^{\bullet-}$ reaction, but considered the sum of $\text{Br}_2^{\bullet-}$ + (unknown) $\text{Cl}_2^{\bullet-}$ processes as accounted for by $\text{Br}_2^{\bullet-}$ alone. Therefore, if $\text{Cl}_2^{\bullet-}$ proves to be actually important

in GSH photodegradation in saltwater, our model prediction for the role of $\text{Br}_2^{\bullet-}$ should be considered as applying to the contributions of $\text{Br}_2^{\bullet-}$ and $\text{Cl}_2^{\bullet-}$ taken together.

Conclusions

Based on our model predictions and on the comparison with the available experimental data, we can conclude that the photodegradation of GSH in freshwaters would be dominated by $\cdot\text{OH}$ at low DOC and by $^3\text{CDOM}^*$ at high DOC. In contrast, the phototransformation of GS^- would be dominated by $\text{CO}_3^{\bullet-}$ at low DOC and by $^1\text{O}_2/^3\text{CDOM}^*$ (as well as H_2O_2) at high DOC. GS^- is more photolabile than GSH, thus the kinetics of GLU ($\text{GSH} + \text{GS}^-$) phototransformation would become faster with increasing pH. The pH increase of the reaction kinetics would be accounted for by $\text{CO}_3^{\bullet-}$ at low DOC and by $^1\text{O}_2$ (and H_2O_2) at high DOC. The most favourable conditions to GLU photodegradation in surface freshwaters imply low DOC and high pH, where $\text{CO}_3^{\bullet-}$ is expected to dominate the photoreactions. Therefore, $\text{CO}_3^{\bullet-}$ is a key transient for the photodegradation of GLU in freshwaters because it predominates where photochemistry is most competitive with biodegradation. Interestingly, high-pH conditions can be obtained in the presence of elevated photosynthetic activity that consumes dissolved CO_2 : this is a good example of synergy between biology and photochemistry, where a biological process ensures the conditions for photochemistry to prevail over microbial degradation. These findings might probably apply as well to other peptidic thiols that behave similarly to GLU (Chu et al., 2017), although their $\text{CO}_3^{\bullet-}$ reaction rate constants are still unknown.

A small salinity level is sufficient to shift the photodegradation pathways of GSH towards $\text{Br}_2^{\bullet-}$, which is thus likely to dominate the GSH phototransformation in brackish- and seawater. Because

an increase in salinity enhances the $\text{Br}_2^{\bullet-}$ process but inhibits the $\bullet\text{OH}$ one, salinity does not necessarily speed up the GSH photodegradation. For an important salinity-induced acceleration to occur, one needs elevated DOC and low nitrate/nitrite levels.

Acknowledgements

Financial support by MIUR-PNRA is gratefully acknowledged.

References

- Avetta, P., Fabbri, D., Minella, M., Brigante, M., Maurino, V., Minero, C., Pazzi, M., Vione, D., 2016. Assessing the phototransformation of diclofenac, clofibric acid and naproxen in surface waters: Model predictions and comparison with field data. *Water Res.* 105, 383-394.
- Bodrato, M., Vione, D., 2014. APEX (Aqueous Photochemistry of Environmentally occurring Xenobiotics): A free software tool to predict the kinetics of photochemical processes in surface waters. *Environ. Sci.: Processes Impacts* 16, 732-740.
- Bortolus, P., Monti, S., Albini, A., Fasani, E., Pietra, S., 1989. Physical quenching and chemical reaction of singlet molecular oxygen with azo dyes. *J. Org. Chem.* 54, 534-540.
- Brigante, M., Minella, M., Mailhot, G., Maurino, V., Minero, C., Vione, D., 2014. Formation and reactivity of the dichloride radical ($\text{Cl}_2^{\bullet-}$) in surface waters: A modelling approach. *Chemosphere* 95, 464-469.
- Buxton, G. V.; Greenstock, C. L.; Helman, W. P.; Ross, A. B., 1988. Critical review of rate constants for reactions of hydrated electrons, hydrogen atoms and hydroxyl radicals ($\bullet\text{OH}/\text{O}^{\bullet-}$) in aqueous solution. *J. Phys. Chem. Ref. Data* 17, 513-886.

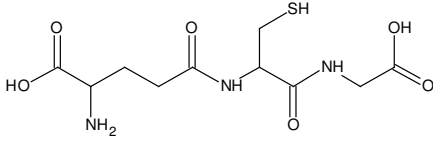
- Canonica, S., Freiburghaus, M., 2001. Electron-rich phenols for probing the photochemical reactivity of freshwaters. *Environ. Sci. Technol.* 35, 690-695.
- Canonica, S., Kohn, T., Mac, M., Real, F.J., Wirz, J., Von Gunten, U., 2005. Photosensitizer method to determine rate constants for the reaction of carbonate radical with organic compounds. *Environ. Sci. Technol.* 39, 9182-9188.
- Chu, C., Stamatelatos, D., McNeill, K., 2017. Aquatic indirect photochemical transformations of natural peptidic thiols: impact of thiol properties, solution pH, solution salinity and metal ions. *Environ. Sci.: Processes Impacts* 19, 1518-1527.
- De Laurentiis, E., Minella, M., Maurino, V., Minero, C., Mailhot, G., Sarakha, M., Brigante, M., Vione, D., 2012. Assessing the occurrence of the dibromide radical ($\text{Br}_2^{\cdot-}$) in natural waters: Measures of triplet-sensitised formation, reactivity, and modelling. *Sci. Total. Environ.* 439, 299-306.
- Dupont, C. L., Moffett, J. W., Bidigare, R. R., Ahner, B. A., 2006. Distributions of dissolved and particulate biogenic thiols in the subarctic Pacific Ocean. *Deep Sea Res. Part I* 53, 1961-1974.
- Encinas, M. V., Lissi, E. A., Olea, A. F., 1985. Quenching of triplet benzophenone by vitamins E and C and by sulfur containing aminoacids and peptides. *Photochem. Photobiol.* 42, 347-352.
- Gligorovski, S., Streckowski, R., Barbati, S., Vione, D., 2015. Environmental implications of hydroxyl radicals ($\cdot\text{OH}$). *Chem. Rev.* 115, 13051-13092.
- Grill, E., Winnacker, E. L., Zenk, M. H., 1985. Phytochelatins: the principal heavy-metal complexing peptides of higher plants. *Science* 230, 674-676.
- Huang, J. P., Mabury, S. A., 2000a. Steady-state concentrations of carbonate radicals in field waters. *Environ. Toxicol. Chem.* 19, 2181-2188.
- Huang, J. P., Mabury, S. A., 2000b. The role of carbonate radical in limiting the persistence of sulfur-containing chemicals in sunlit natural waters. *Chemosphere* 41, 1775-1782.
- Hurley, J. K., Linschitz, H., Treinin, A., 1988. Interaction of halide and pseudohalide ions with triplet benzophenone-4-carboxylate: Kinetics and radical yields. *J. Phys. Chem.* 92, 5151-5159.

- Ibarra, C., Nieslanik, B. S., Atkins, W. M., 2001. Contribution of aromatic–aromatic interactions to the anomalous pK_a of tyrosine-9 and the C-terminal dynamics of glutathione *S*-transferase A1-1. *Biochemistry* 40, 10614-10624.
- Kieber, D. J., Miller, G. W., Neale, P. J., Mopper, K., 2014. Wavelength and temperature-dependent apparent quantum yields for photochemical formation of hydrogen peroxide in seawater. *Environ. Sci.: Processes Impacts* 16, 777-791.
- Lee, K., Tong, L. T., Millero, F. J., Sabine, C. L., Dickson, A. G., Goyet, C., Park, G. H., Wanninkhof, R., Feely, R. A., Key, R. M., 2006. Global relationships of total alkalinity with salinity and temperature in surface waters of the world's oceans. *Geophys. Res. Lett.* 33, L19605.
- Leggatt, R. A., Brauner, C. J., Schulte, P. M., Iwama, G. K., 2007. Effects of acclimation and incubation temperature on the glutathione antioxidant system in killifish and RTH-149 cells. *Compar. Biochem. Physiol. A* 146, 317-326.
- Marchisio, A., Minella, M., Maurino, V., Minero, C., Vione, D., 2015. Photogeneration of reactive transient species upon irradiation of natural water samples: Formation quantum yields in different spectral intervals, and implications for the photochemistry of surface waters. *Water Res.* 73, 145-156.
- Martell, A.E., Smith, R.M., Motekaitis, R.J., 1997. Critically Selected Stability Constants Of Metal Complexes Database, Version 4.0.
- McKay, G., Rosario-Ortiz, F. L., 2016. Photochemical reactivity of organic matter and its size fractions. In: *Surface Water Photochemistry*, Calza, P. and Vione, D. (Eds.), RSC Publishing, London, pp. 77-95.
- McNeill, K., Canonica, S., 2016. Triplet state dissolved organic matter in aquatic photochemistry: Reaction mechanisms, substrate scope, and photophysical properties. *Environ. Sci.: Processes Impacts* 18, 1381-1399.

- Mezyk, S. P., 1996. Rate constant determination for the reaction of hydroxyl and glutathione thiyl radicals with glutathione in aqueous solution. *J. Phys. Chem.* 100, 8861-8866.
- Minella, M., Rapa, L., Carena, L., Pazzi, M., Maurino, V., Minero, C., Brigante, M., Vione, D., in press. Experimental methodology to measure the reaction rate constants of processes sensitised by the triplet state of 4-carboxybenzophenone as proxy of the triplet states of chromophoric dissolved organic matter, under steady-state irradiation conditions. *Environ. Sci.: Processes Impacts*, DOI: 10.1039/C8EM00155C.
- Mostofa, K. M. G., Liu, C. Q., Zhai, W. D., Minella, M., Vione, D., Gao, K. S., Minataka, D., Arakaki, T., Yoshioka, T., Hayakawa, K., Konohira, E., Tanoue, E., Akhand, A., Chanda, A., Wang, B., Sakugawa, H., 2016. Reviews and Syntheses: Ocean Acidification and its Potential Impacts on Marine Ecosystems. *Biogeosciences* 13, 1767-1786.
- Neta, P., Huie, R. E., Ross, A. B., 1988. Rate constants for reactions of inorganic radicals in aqueous solution. *J. Phys. Chem. Ref. Data* 17, 1027-1284.
- Parker, K. M., Mitch, W.A., 2016. Halogen radicals contribute to photooxidation in coastal and estuarine waters. *Proc. Natl. Acad. Sci. USA* 113, 5868-5873.
- Paulsen, C. E., Carroll, K. S., 2013. Cysteine-mediated redox signaling: Chemistry, biology, and tools for discovery. *Chem. Rev.* 113, 4633-4679.
- Powers, L. C., Miller, W. L., 2014. Blending remote sensing data products to estimate photochemical production of hydrogen peroxide and superoxide in the surface ocean. *Environ. Sci.: Processes Impacts* 16, 792-806.
- Richard, C., Hoffmann, N., 2016. Direct photolysis processes. In: *Surface Water Photochemistry*, Calza, P. and Vione, D. (Eds.), RSC Publishing, London, pp. 61-75.
- Rosario-Ortiz, F. L., Canonica, S., 2016. Probe compounds to assess the photochemical activity of dissolved organic matter. *Environ. Sci. Technol.* 50, 12532-12547.

- Sur, B., Rolle, M., Minero, C., Maurino, V., Vione, D., Brigante, M., Mailhot, G., 2011. Formation of hydroxyl radicals by irradiated 1-nitronaphthalene (1NN): Oxidation of hydroxyl ions and water by the 1NN triplet state. *Photochem. Photobiol. Sci.* 10, 1817-1824.
- Swarr, G. J., Kading, T., Lamborg, C. H., Hammerschmidt, C. R., Bowman, K. L., 2016. Dissolved low-molecular weight thiol concentrations from the U.S. GEOTRACES North Atlantic Ocean zonal transect. *Deep Sea Res. Part I* 116, 77-87.
- Trogolo, D., 2016. Quantum chemical studies of reactive species in water. PhD thesis, Ecole Polytechnique Federale de Lausanne (EPFL). <https://infoscience.epfl.ch/record/223526>, last accessed January 2018.
- Vione, D., Minella, M., Maurino, V., Minero, C., 2014. Indirect photochemistry in sunlit surface waters: Photoinduced production of reactive transient species. *Chemistry Eur. J.* 20, 10590-10606.
- Von Gunten, U., Hoigné, J., 1996. Ozonation of bromide-containing waters: Bromate formation through ozone and hydroxyl radicals. In: *Disinfection By-Products in Water Treatment*, Minear, R. A., Amy, G. L. (eds.), CRC Press, Boca Raton, FL, pp. 187-206.
- Wei, L. P., Ahner, B. A., 2005. Sources and sinks of dissolved phytochelatin in natural seawater. *Limnol. Oceanogr.* 50, 13-22.
- Wetzel, R. G., 2001. *Limnology: Lake and River Ecosystems*. 3rd edition, Academic Press.
- Wilkinson, F., Helman W. P., Ross, A. B., 1995. Rate constants for the decay and reactions of the lowest electronically excited singlet state of molecular oxygen in solution. *J. Phys. Chem. Ref. Data* 24, 663-1021.
- Zehavi, D., Rabani, J., 1972. The oxidation of aqueous bromide ions by hydroxyl radicals. A pulse radiolytic investigation. *J. Phys. Chem.* 76, 312-319.

Table 1. Indirect photoreactivity parameters of GLU (GSH + GS⁻, with the two species considered separately). Note the higher reactivity of electron-rich GS⁻ towards ¹O₂ and CO₃^{•-}, and the higher reactivity of GSH towards [•]OH.

	 GLU		
x = GSH or GS⁻	GSH	GS⁻	Reference
$k_{x, \bullet\text{OH}}, \text{L mol}^{-1} \text{s}^{-1}$	3.5×10^9	9.0×10^8	Buxton et al., 1988
$k_{x, {}^1\text{O}_2}, \text{L mol}^{-1} \text{s}^{-1}$	2.4×10^6	2.1×10^8	Chu et al., 2017
$k_{x, {}^3\text{BP}^*}, \text{L mol}^{-1} \text{s}^{-1}$	6.7×10^8	6.7×10^8	Encinas et al., 1985 (quenching)
$k_{x, {}^3\text{CDOM}^*}, \text{L mol}^{-1} \text{s}^{-1}$	8×10^7	8×10^7	This work (reaction)
$k_{x, \text{CO}_3^{\bullet-}}, \text{L mol}^{-1} \text{s}^{-1}$	5.3×10^6	7.1×10^8	Neta et al., 1988
$k_{x, \text{Br}_2^{\bullet-}}, \text{L mol}^{-1} \text{s}^{-1}$	2×10^8	n/a	Neta et al., 1988

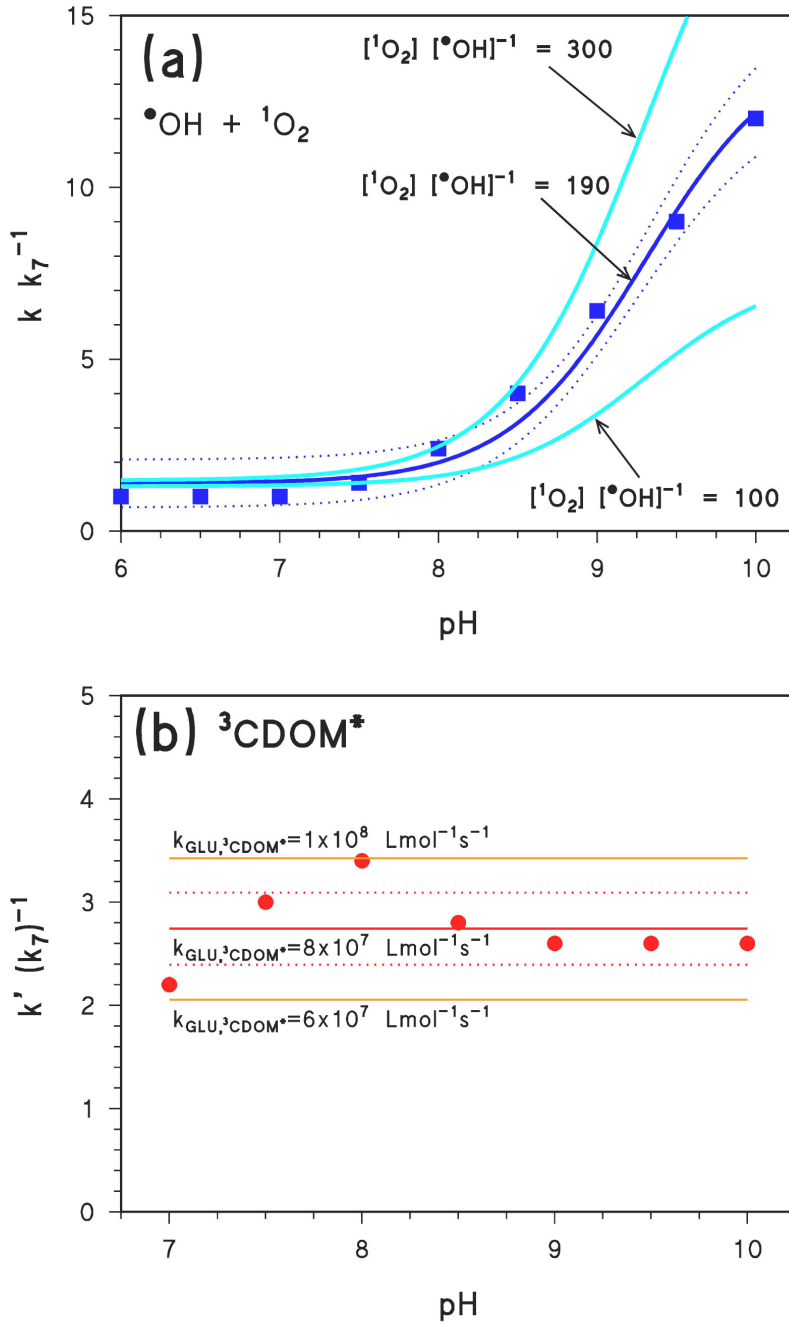
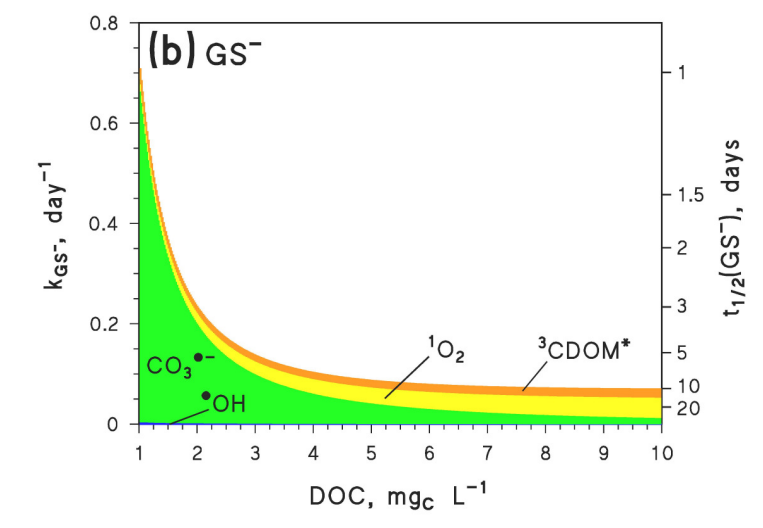
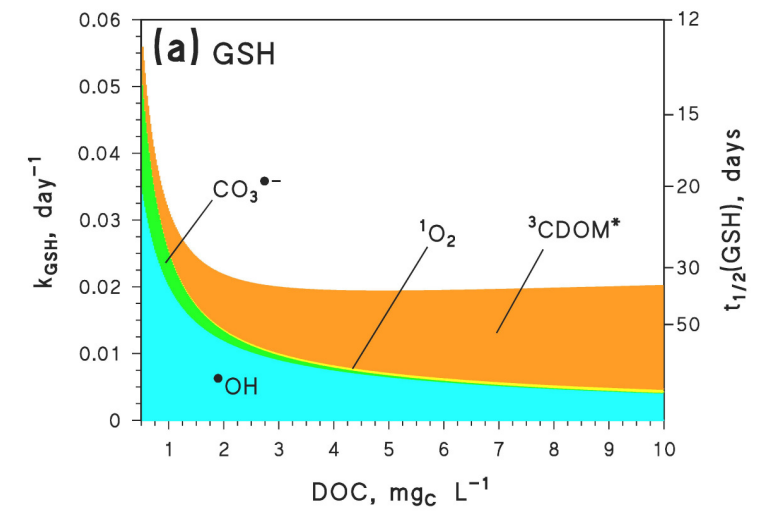


Figure 1. (a) Photochemical model reproduction of the experimental data reported by Chu et al. (2017) for the first-order photodegradation rate constant of GLU (GSH + GS⁻) accounted for by •OH and ¹O₂, as a function of pH. The model prediction is the solid curve, while the dotted curves delimit the 95% confidence band of data fit. The other solid curves represent the model predictions for different values of the [¹O₂] [•OH]⁻¹ ratio. (b) Similar as above, but here the first-order rate constant is referred to unknown pathways in Chu et al. (2017), here interpreted as the ³CDOM* reaction. The solid line is the model prediction, with the 95% confidence band delimited by the dotted lines. The other solid lines show model predictions for different values of $k_{GLU,^3CDOM^*}$.

In both cases, the rate constants were normalised to the first-order rate constant of GLU degradation by ¹O₂ + •OH at pH 7 (k_7).



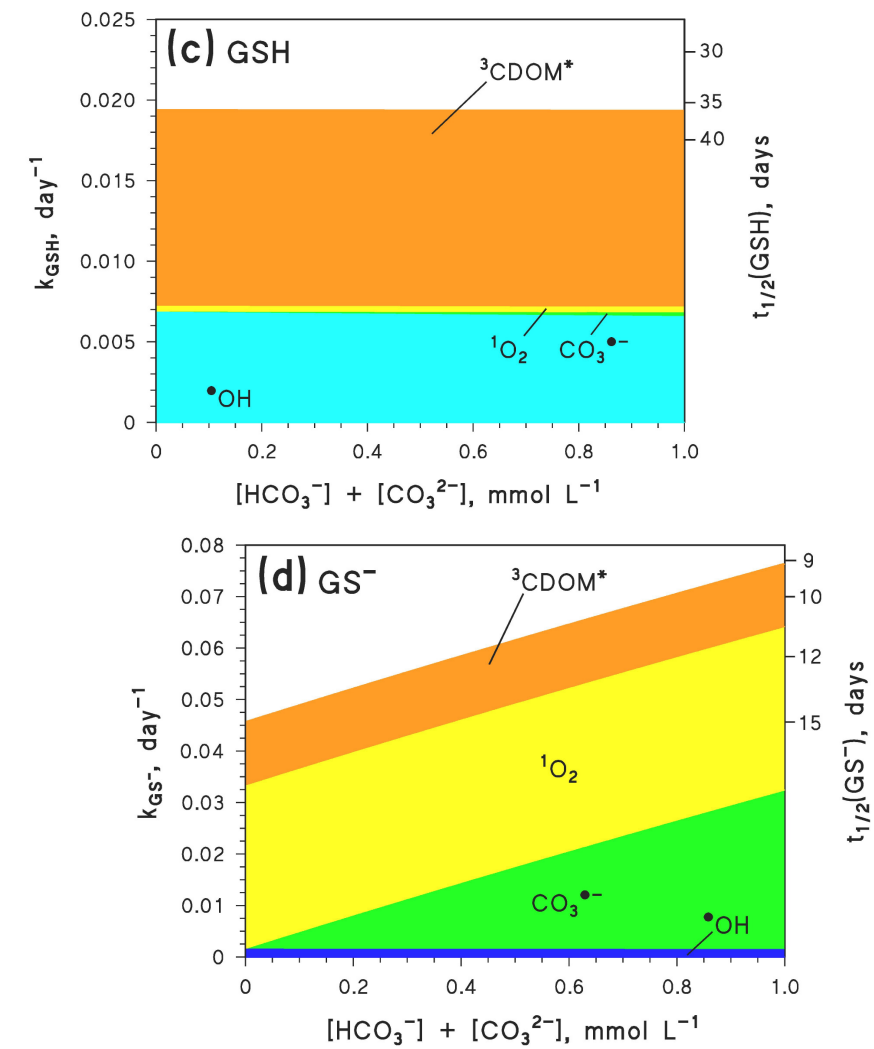


Figure 2. Modelled first-order rate constants of GSH and GS⁻ photodegradation. Each plot shows the overall rate constant, together with the contributions of the different pathways (•OH, CO₃^{•-}, ¹O₂ and ³CDOM*). The rate constants are referred to: **(a)** GSH as a function of DOC; **(b)** GS⁻ as a function of DOC; **(c)** GSH as a function of [HCO₃⁻] + [CO₃²⁻] (with [CO₃²⁻] = 0.01 [HCO₃⁻], pH ~8.3); **(d)** GS⁻ as a function of [HCO₃⁻] + [CO₃²⁻]. The half-life times of GSH and GS⁻ ($t_{1/2} = \ln 2 k^{-1}$) are also reported in the right Y-axes. Other water conditions: 5 m water depth, 0.1 mmol L⁻¹ nitrate, 1 μmol L⁻¹ nitrite. In (a,b) there is also 1 mmol L⁻¹ bicarbonate and 10 μmol L⁻¹ carbonate, in (c,d) it is DOC = 5 mg_C L⁻¹.

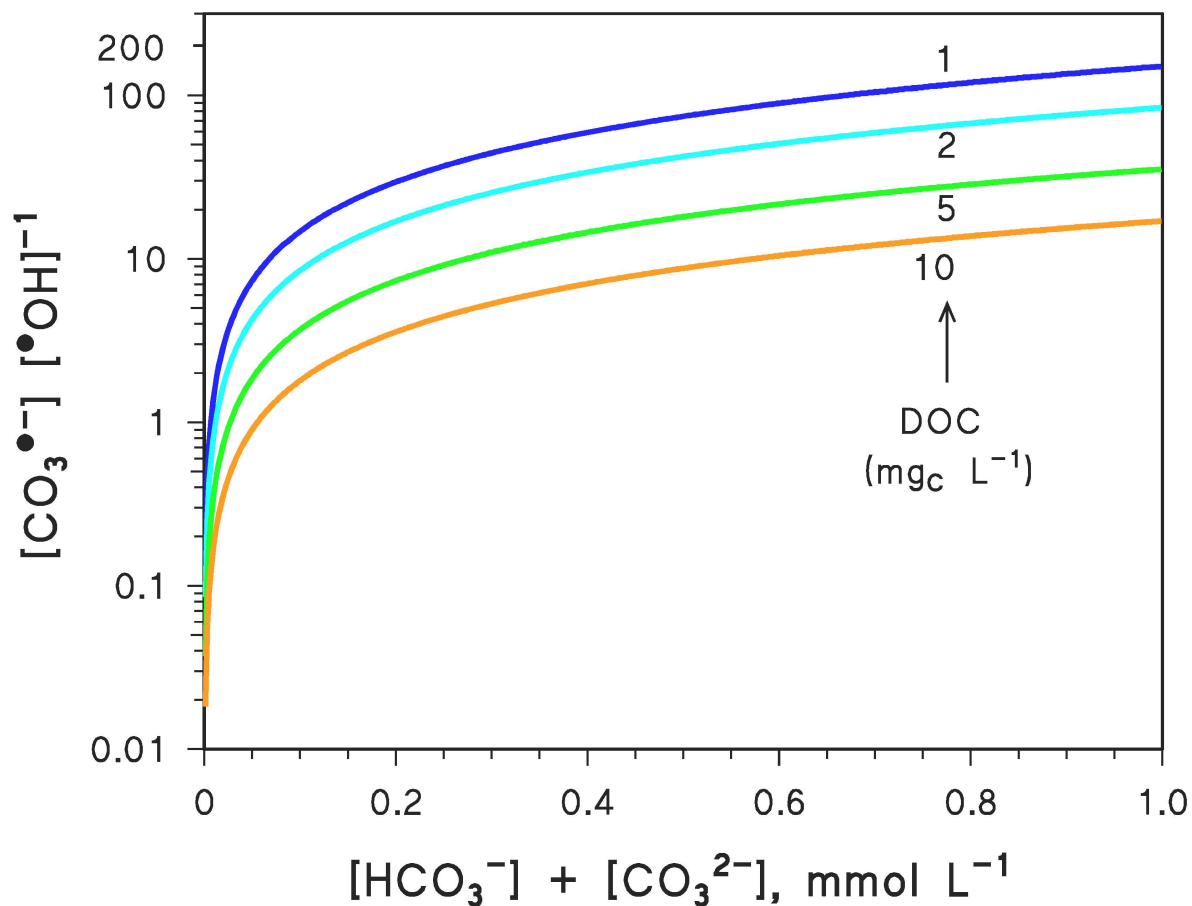


Figure 3. Modelled steady-state concentration ratio $[\text{CO}_3^{\bullet-}] [\bullet\text{OH}]^{-1}$, referred to 22 W m^{-2} sunlight UV irradiance, as a function of $[\text{HCO}_3^-] + [\text{CO}_3^{2-}]$ (with $[\text{CO}_3^{2-}] = 0.01 [\text{HCO}_3^-]$, pH ~ 8.3) and for different DOC values (reported near each curve). Other water conditions: 5 m depth, 0.1 mmol L^{-1} nitrate, $1 \mu\text{mol L}^{-1}$ nitrite.

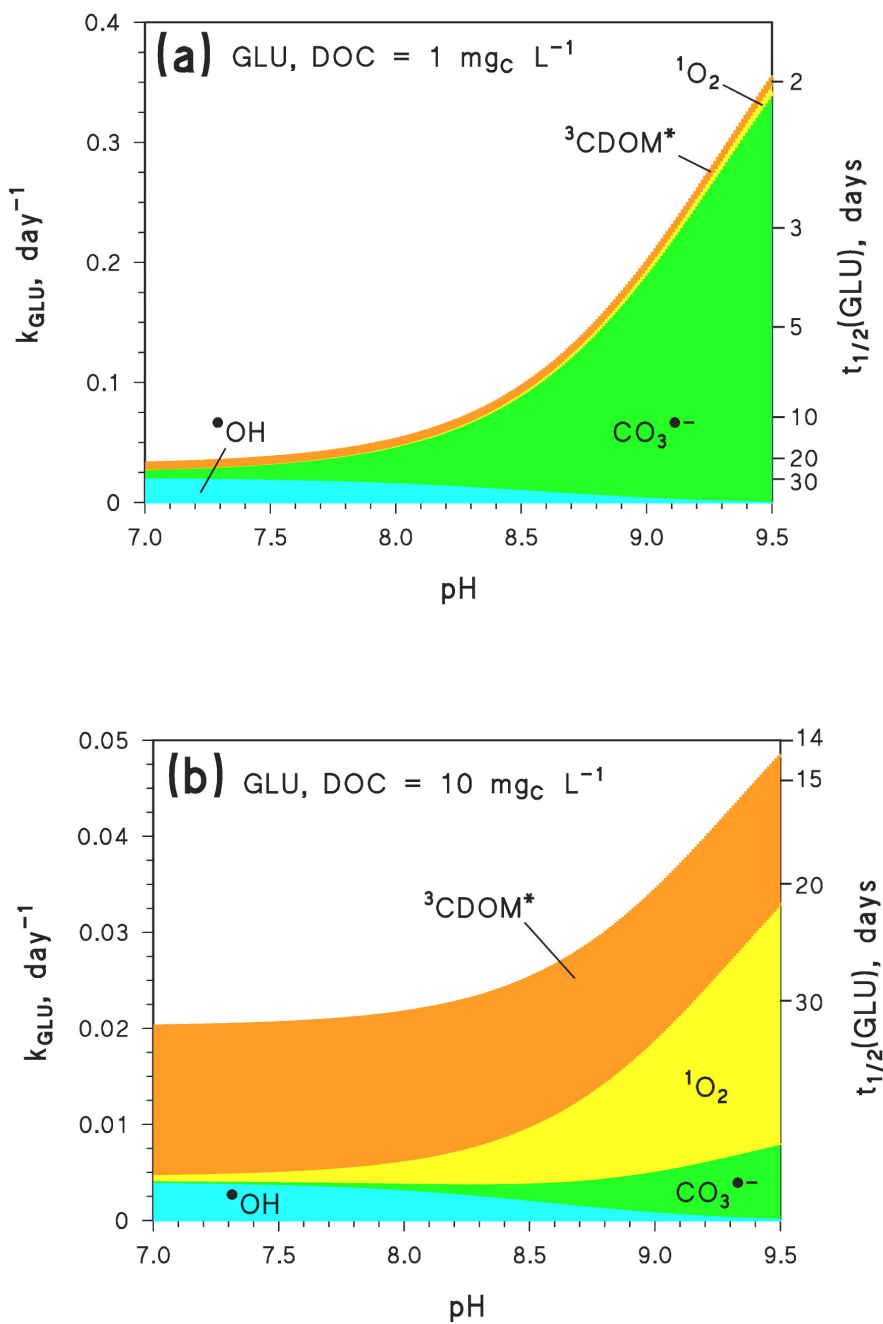


Figure 4. Modelled first-order rate constants of GLU ($\text{GSH} + \text{GS}^-$) photodegradation as a function of pH, for (a) $\text{DOC} = 1 \text{ mg}_C \text{ L}^{-1}$ and (b) $\text{DOC} = 10 \text{ mg}_C \text{ L}^{-1}$. Each plot shows the overall rate constant, together with the contributions of the different pathways ($\bullet\text{OH}$, $\text{CO}_3^{\bullet-}$, $^1\text{O}_2$ and $^3\text{CDOM}^*$). Other water conditions: 5 m water depth, 0.1 mmol L^{-1} nitrate, $1 \mu\text{mol L}^{-1}$ nitrite, 1 mmol L^{-1} bicarbonate and $10 \mu\text{mol L}^{-1}$ carbonate. The GLU half-life times ($t_{1/2} = \ln 2 k^{-1}$) are also reported in the right Y-axes.

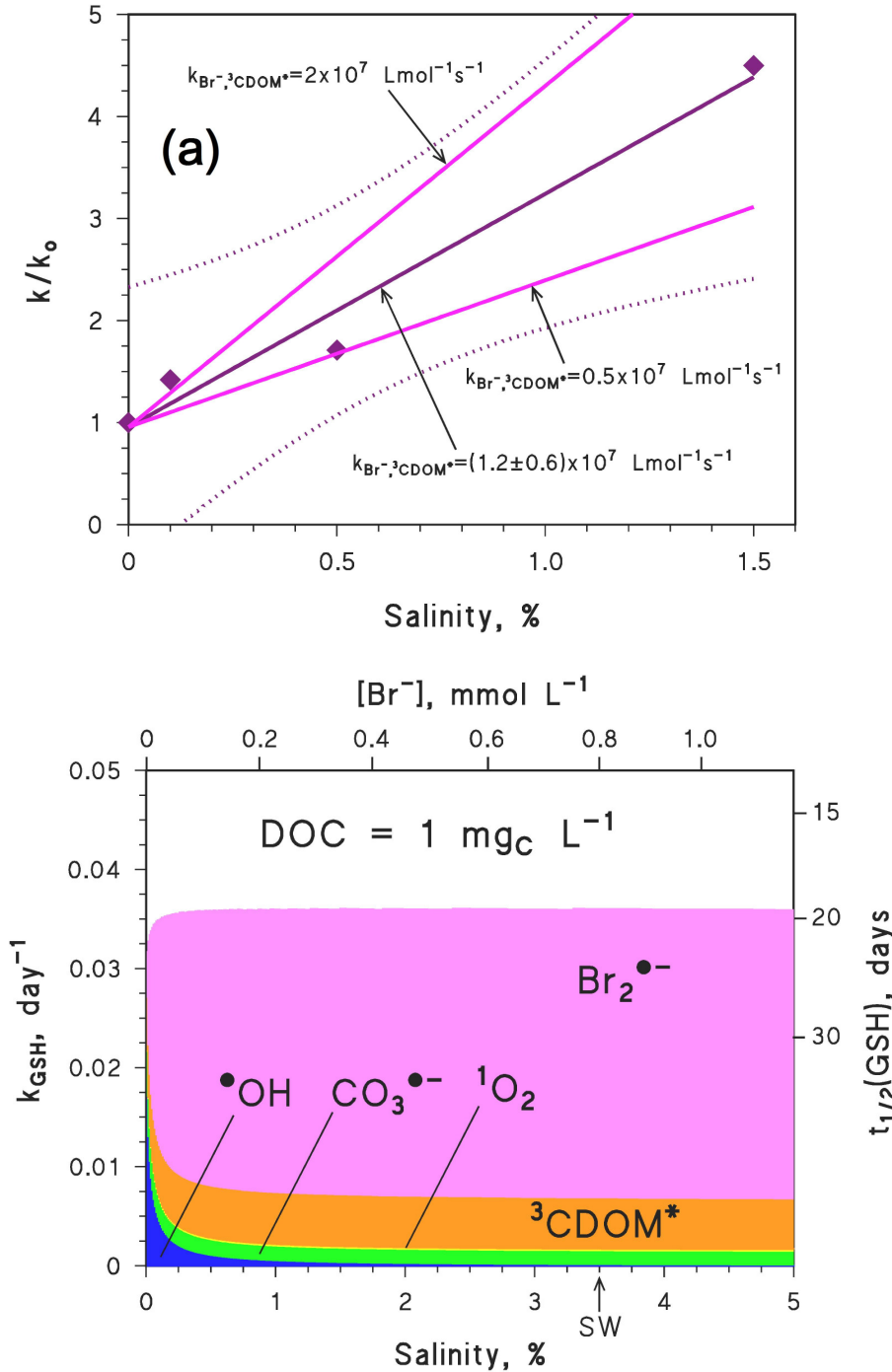


Figure 5. (a) Photochemical model reproduction of the experimental data reported by Chu et al. (2017) for the first-order photodegradation rate constant of GSH as a function of salinity. The model prediction is the solid line, while the dotted lines delimit the 95% confidence band of data fit. The other solid lines represent the model predictions for different values of the $k_{Br^-,^3CDOM^*}$ rate constant.

(b) Modelled first-order rate constant of GSH photodegradation as a function of salinity. The plot shows the overall rate constant, together with the contributions of the different pathways ($^{\bullet}\text{OH}$, $\text{CO}_3^{\bullet-}$, $^1\text{O}_2$ and $^3\text{CDOM}^*$). Other water conditions: 5 m water depth, 0.1 mmol L^{-1} nitrate, $1 \text{ } \mu\text{mol L}^{-1}$ nitrite, 1 mmol L^{-1} bicarbonate and $10 \text{ } \mu\text{mol L}^{-1}$ carbonate. The GLU half-life times ($t_{1/2} = \ln 2 / k^{-1}$) are also reported in the right Y-axis, and bromide concentration in the upper X-axis.